

Memo on CSR emittance dilution in Bates magnets (Dec, 2001)

I.V. Bazarov

Wilson lab, Cornell University, Ithaca, NY 14853

Abstract

This memo contains a first-cut study of CSR in the Bates magnets. Bunch compression with Bates magnets is discussed.

Bates system

JLAB Demo FEL's "Bates" achromat is shown in Fig. 1. It consists of five dipoles ($2\times B1$, $2\times B2$, $B3$), 4 sextupoles ($2\times S1$, $2\times S2$) and 4 quads ($2\times Q1$, $2\times Q2$).

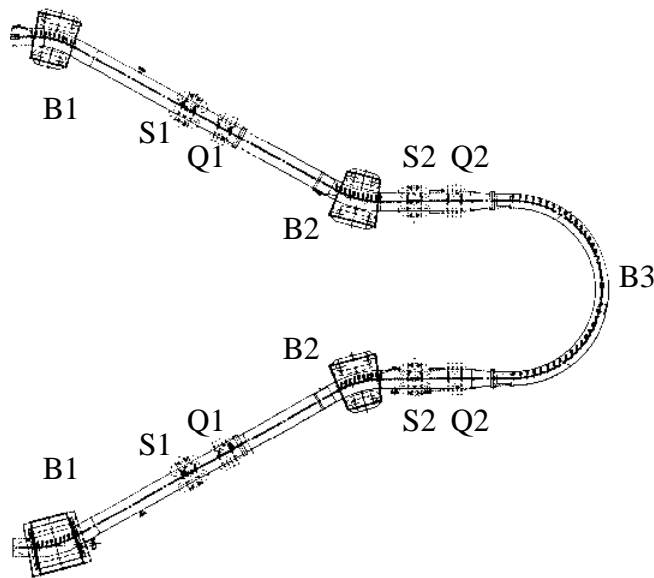


Fig. 1. Bates achromat from JLAB Demo IR-FEL.

$B1$ and $B2$ dipoles have 29.38° bending angle, $B3$ bends 180° and all magnets have bending radius of 1 m. $B1$ and $B2$ have face pole rotation angles of 10.79° and 6.43° respectively (entrance and exit poles are rotated by the same angle in TRANSPORT notations). $B3$ is a sector magnet.

The optical properties of the system are achieved by dipoles configuration alone and quadrupoles (trim quads) are used only to modify characteristics of this achromat such as momentum compaction (R_{56}). Sextupoles are used to change second-order momentum compaction (T_{566}) and aberrations in the Bates. Because of negative bend $B2$ both positive and negative R_{56} values are achievable with the trim quads. Besides, two kicks of opposite signs just before and after the π -bend (not shown) allow path length adjustment.

Bunch length in the Bates

From the entrance of the system, 0, to some point t in it we have the mapping of 6 phase space coordinates:

$$\begin{pmatrix} x \\ x' \\ y \\ y' \\ l \\ \delta \end{pmatrix}_t = \begin{pmatrix} R_{11} & R_{12} & 0 & 0 & R_{16} \\ R_{21} & R_{22} & 0 & 0 & R_{26} \\ 0 & 0 & R_{33} & R_{34} & 0 \\ 0 & 0 & R_{43} & R_{44} & 0 \\ R_{51} & R_{52} & 0 & 0 & R_{56} \\ 0 & 0 & 0 & 0 & 1 \end{pmatrix} \begin{pmatrix} x \\ x' \\ y \\ y' \\ l \\ \delta \end{pmatrix}_0$$

R_{16} and R_{26} are dispersion η_x and its derivative η'_x respectively; $R_{51} = \int_0^t R_{11}(\tau)h(\tau)d\tau$ and $R_{52} = \int_0^t R_{21}(\tau)h(\tau)d\tau$ ($h(\tau)=1/\rho(\tau)$, ρ is bending radius); and the other elements have their usual meaning. Outside of achromat, where $\eta_x = \eta'_x = 0$, we have $R_{51} = R_{52} = 0$. R_{51} , R_{52} , and R_{56} in the Bates are shown in Fig. 2.

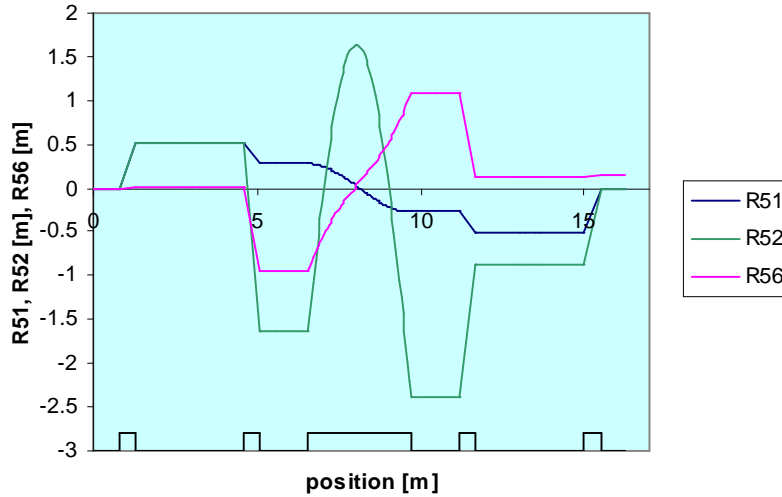


Fig. 2. R_{51} , R_{52} , and R_{56} in the Bates when quads are turned off. Positions of the dipoles are shown.

Assuming that we have in the bunch $\delta = \alpha_\delta l$, with δ - l correlation coefficient

$\alpha_\delta = -\frac{E_{\text{cav}} \sin \varphi}{E_0} \frac{1}{\Delta_{\text{RF}}}$ (here φ is off-crest RF phase, E_{cav} is RF energy gain when on-crest, $E_0 = 100$ MeV, $\Delta_{\text{RF}} = \lambda_{\text{RF}}/2\pi$, λ_{RF} is RF wavelength) we can write for rms

horizontal, vertical and longitudinal bunch size:

$$\begin{aligned}\sigma_{x,t}^2 &= \varepsilon_x \beta_{x,t} + \alpha_\delta^2 \eta_{x,t}^2 \sigma_{l,0}^2, \\ \sigma_{y,t}^2 &= \varepsilon_y \beta_{y,t}, \\ \sigma_{l,t}^2 &= \sigma_{l,0}^2 (1 + \alpha_\delta R_{56})^2 + \varepsilon_x (\beta_{x,0} R_{51}^2 - 2\alpha_{x,0} R_{51} R_{52} + \gamma_{x,0} R_{52}^2),\end{aligned}\quad (1)$$

here β_x , α_x , γ_x , ε_x and β_y , α_y , γ_y , ε_y are usual Twiss parameters (at the Bates entrance for subscript $_0$, or inside the Bates for subscript $_t$). For all simulations I have assumed initial bunch length (after the main linac) to be $\sigma_{l,0} = 0.6$ mm and normalized rms emittance $\varepsilon_{n,x} = \varepsilon_{n,y} = 1$ mm-mrad. It turns out that the second term in (1) is usually small in comparison with the first one as $\varepsilon_x = \varepsilon_{n,x} / \beta\gamma = 5.1 \cdot 10^{-9}$ m, so the bunch length is given by $\sigma_{l,0} |1 + \alpha_\delta R_{56}|$ with exception of the point of maximum compression ($R_{56} = -1/\alpha_\delta$). In the π -bend R_{56} changes from about -1 m to 1 m, so the bunch goes through longitudinal cross-over in there (for $|\alpha_\delta| \geq 1 \text{ m}^{-1}$ or $|\varphi| > 2.2^\circ$) and possibly in one of the shorter bends too depending on φ and final R_{56} . The consequences of such crossovers are not so explicit with respect to CSR. On one hand, very short bunches in a bend are significant sources of CSR, but the bunch gets very short only over a small distance in the bend and becomes larger than $\sigma_{l,0}$ in other parts, thus, CSR wake may not have sufficient time to build up. On the other hand, by operating on-crest ($\alpha_\delta = 0$) the bunch length stays approximately the same, but because of rather short initial bunch length of 0.6 mm one may expect to see some CSR wake to build up over the π -bend. This becomes clearer as we discuss TraFiC4 results below. An examples of bunch lengths in the Bates is shown in Fig. 3 for RF offset φ in the main linac equal to -10 , 0 , 10° (quads are turned off, $R_{56} = 14.4$ cm). Second term in (1) is also plotted.

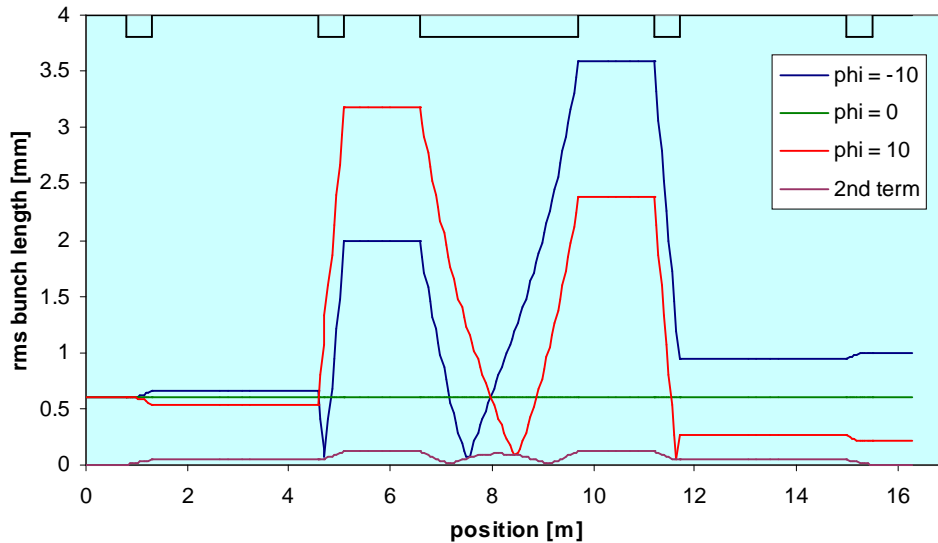


Fig. 3. Bunch length in the Bates (trim quads are turned off, $R_{56} = 14.4$ cm). Initial bunch length is 0.6 mm. The second term in (1) is also shown.

Changing R_{56} in the Bates

R_{56} can be changed in a wide range with the trim quads. See Fig. 4. An example of changes in optical functions is shown in Fig. 5.

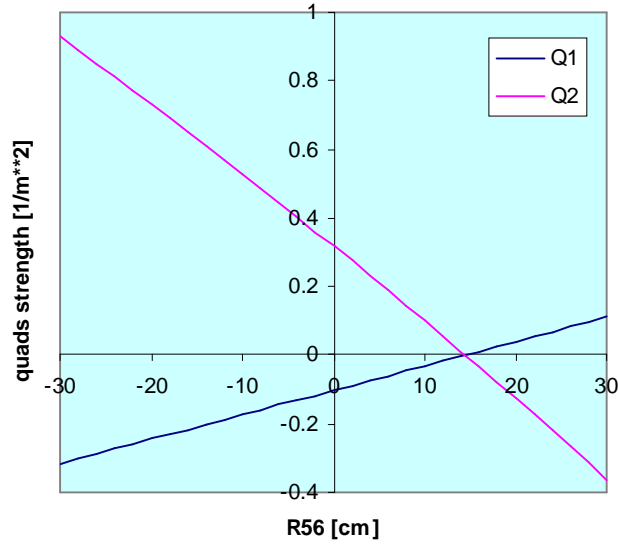


Fig. 4. Trim quads strength in the Bates to achieve certain R_{56} .

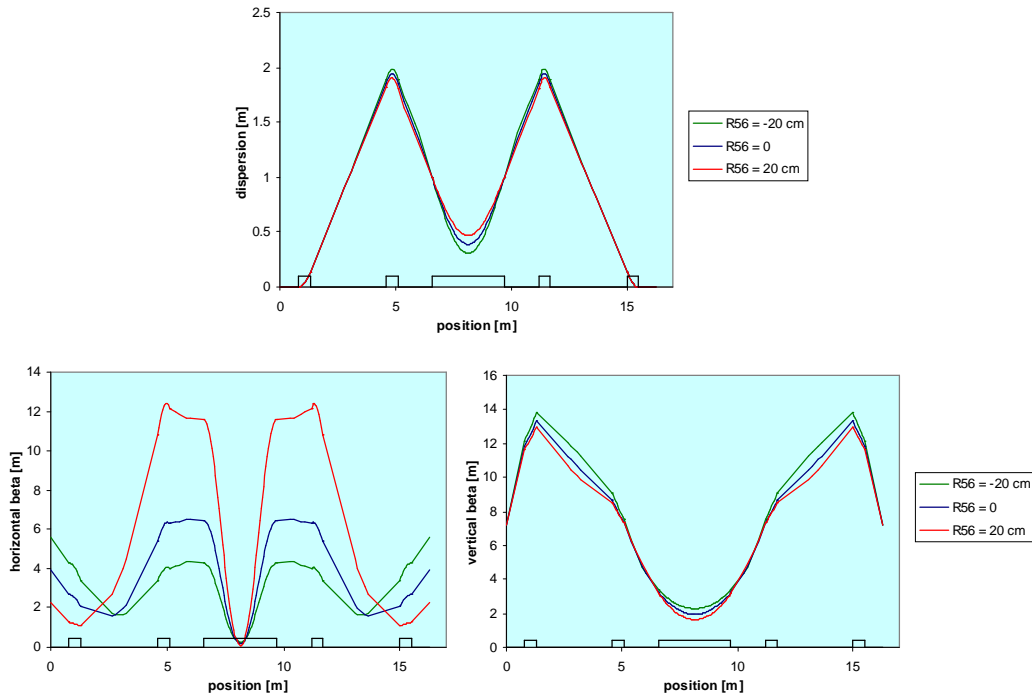


Fig. 5. Changes in optical functions for various values of R_{56} . In case of β_x , $\alpha_{x,0}$ is fixed; and in case of β_y plot, $\beta_{y,0}$ is fixed.

TraFiC4 results

The system was simulated with TraFiC4 [<http://www.slac.stanford.edu/~akabel/TraFiC4>]. The number of bunchlets was 300, distribution was Gaussian in all three directions, longitudinal phase space occupied a small portion of the RF cosine waveform and included initial uncorrelated energy spread from the injector (10 keV, rms). The transport line was “sliced” into about 200 sections (each about 10 cm long). The code stores the history of the bunch in all these slices to be able to calculate retarded fields responsible for CSR effect. One run takes about 3-4 hours on 500 MHz Unix station.

In these simulations, both sextupoles and quadrupoles in the Bates are turned off, thus, $R_{56} = 14.4$ cm. Sextupole element appears to work incorrectly in the code, as turning on of sextupoles changes R_{56} of the system. Fig. 6 shows emittance growth from the Bates as a function of RF phase offset φ . Fig. 7 shows rms bunch length after the Bates as a function of φ . Fig. 8 shows rms energy spread vs. φ . In all cases final beam energy was forced to 100 MeV. Error bars on the plots correspond to statistical error of $1/\sqrt{N} = 5.8$ % (N is number of bunchlets).

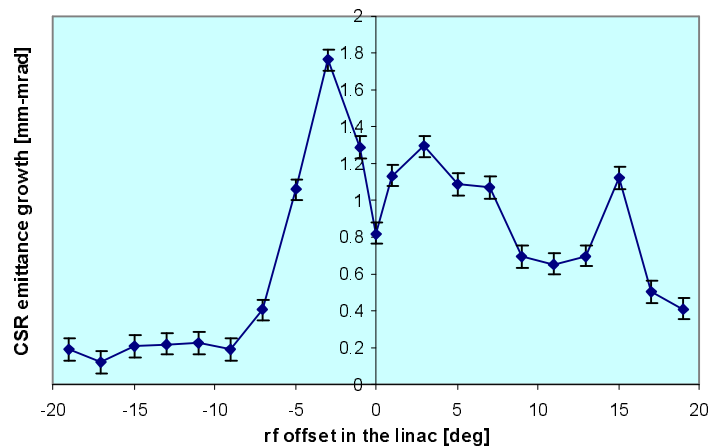


Fig. 6. Emittance growth from the Bates vs. RF offset φ . Error bars correspond to $1/\sqrt{N} = 5.8$ % of initial 1 mm-mrad emittance.

By comparing these three graphs it is possible to explain CSR emittance growth from the Bates. When operating significantly off-crest, δ - l correlation coefficient α_δ and energy spread σ_δ are large, thus, bunch gets compressed in two points in the Bates (see Fig. 3), but is long everywhere else in the dipoles. As a result, CSR wake does not have sufficient time to build up and emittance growth from Bates is small at the expense of larger energy spread. It is also clear that for $\varphi < 0$ ($\alpha_\delta > 0$) smaller emittance growth takes place for the same absolute value of φ (for $R_{56} < 0$ it will be the opposite). Now, as

the main linac is operated closer to the on-crest point, α_δ and σ_δ become smaller, and longitudinal crossovers still occur, but now the bunch stays short over longer distances in the dipoles, as well as the bunch is shorter overall in the Bates. That corresponds to significant CSR emittance growth for smaller $|\varphi|$ in Fig. 6. The local minimum at $\varphi = 0$ reflects the fact that while the bunch length stays rather short throughout the dipoles at about 0.6 mm, there are no longitudinal crossovers to generate more CSR. At about $\varphi = 15^\circ$, when $\alpha_\delta = -1/R_{56}$, the bunch is maximally compressed in the last dipole (and it is short in the previous one as well), with implications of more CSR in the these last two magnets. That corresponds to the local maximum on Fig. 6 at $\varphi = 15^\circ$.

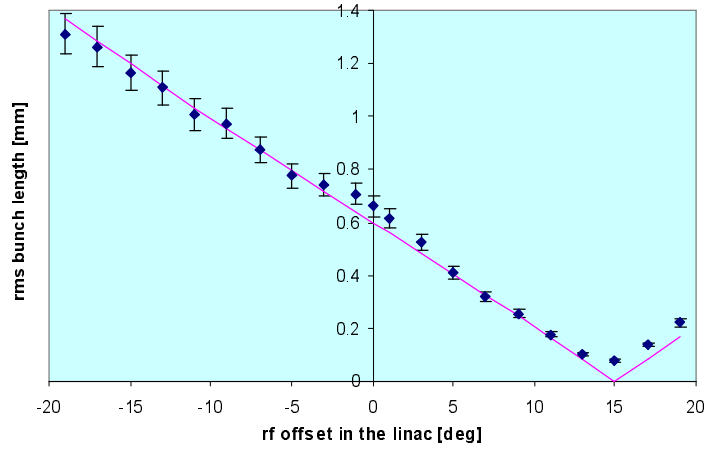


Fig. 7. Bunch length after the Bates vs. RF offset φ . Error bars correspond to $1/\sqrt{N} = 5.8\%$. The curve represents $\sigma_{l,0}|1 + R_{56}\alpha_\delta|$.

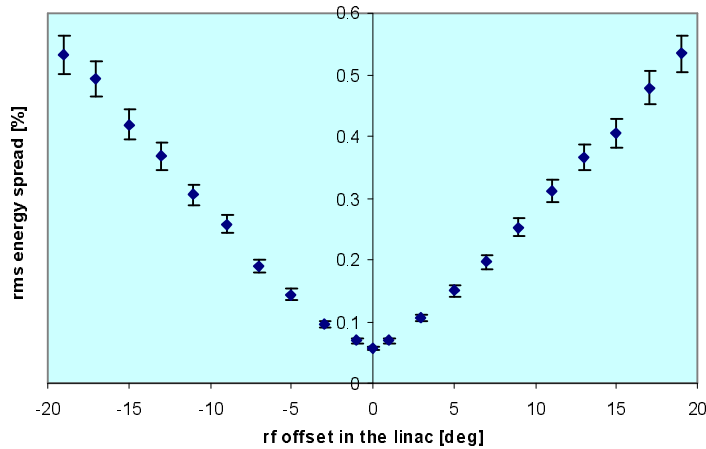


Fig. 8. Energy spread vs. RF offset φ .

Summary

At this point, Bates optics appear to be acceptable for ERL Phase I purposes. By operating largely off-crest, we should be able to preserve low emittance. By scanning RF offset phase φ , we should be able to verify codes' predictions of CSR effect. By changing R_{56} , we should be able to study ultra-short bunches without the need of additional chicanes. Further compression to 100 fs bunches or shorter will require sextupole corrections in the Bates. The study of ring optics properties, including the second order effects by particle tracking, now becomes my primary focus.